Cell Metabolism
Article

The Nuclear Receptor ERRα Is Required for the Bioenergetic and Functional Adaptation to Cardiac Pressure Overload

Janice M. Huss,[1,2,6] Ken-ichi Imahashi,[4,7] Catherine R. Dufour,[5] Carla J. Weinheimer,[1,2] Michael Courtois,[1,2] Atilla Kovacs,[1,2] Vincent Giguère,[5] Elizabeth Murphy,[4,8] and Daniel P. Kelly[1,2,3,*]
[1] Center for Cardiovascular Research
[2] Department of Medicine
[3] Department of Molecular Biology & Pharmacology and Department of Pediatrics
Washington University School of Medicine, St. Louis, MO 63110, USA
[4] Laboratory of Signal Transduction, National Institute of Environmental Health Science, NIH, Research Triangle Park, NC 27709, USA
[5] Molecular Oncology, McGill University Health Centre, Montreal, PQ H3A 1A1, Canada
[6] Present address: Department of Gene Regulation and Drug Discovery, City of Hope, Duarte, CA 91010, USA.
[7] Present address: Takeda Pharmaceutical Company, Ltd., Osaka 540-8645 Japan.
[8] Present address: NHLBI, NIH, Bethesda, MD, 90892, USA.
*Correspondence: dkelly@im.wustl.edu
DOI 10.1016/j.cmet.2007.06.005

SUMMARY

Downregulation and functional deactivation of the transcriptional coactivator PGC-1α has been implicated in heart failure pathogenesis. We hypothesized that the estrogen-related receptor α (ERRα), which recruits PGC-1α to metabolic target genes in heart, exerts protective effects in the context of stressors known to cause heart failure. *ERRα*$^{-/-}$ mice subjected to left ventricular (LV) pressure overload developed signatures of heart failure including chamber dilatation and reduced LV fractional shortening. ^{31}P-NMR studies revealed abnormal phosphocreatine depletion in *ERRα*$^{-/-}$ hearts subjected to hemodynamic stress, indicative of a defect in ATP reserve. Mitochondrial respiration studies demonstrated reduced maximal ATP synthesis rates in *ERRα*$^{-/-}$ hearts. Cardiac ERRα target genes involved in energy substrate oxidation, ATP synthesis, and phosphate transfer were downregulated in *ERRα*$^{-/-}$ mice at baseline or with pressure overload. These results demonstrate that the nuclear receptor ERRα is required for the adaptive bioenergetic response to hemodynamic stressors known to cause heart failure.

INTRODUCTION

The adult heart undergoes distinct forms of hypertrophic growth. Physiologic hypertrophy, during postnatal development or with endurance training ("runner's heart"), enhances functional capacity through coordinated increases in cardiac mass and O_2 consumption, thereby matching mitochondrial respiratory capacity with energetic demand (Strøm et al., 2005). Pathophysiologic stressors, such as chronic pressure or volume overload, induce hypertrophic growth accompanied by a dissociation of increased cardiac mass and workload from available energy reserves (Anversa et al., 1978; Kayar and Weiss, 1992). Pathologic hypertrophy predisposes to cardiac dysfunction and failure through a remodeling process that is incompletely understood. Whereas pathologic hypertrophy is an independent risk factor for future heart failure and death (Vakili et al., 2001), physiologic hypertrophy may be cardioprotective. Characterization of distinct regulatory pathways involved in adaptive versus maladaptive hypertrophic remodeling may reveal novel therapeutic targets for heart failure.

Discrete molecular signatures distinguish pathologic from physiologic cardiac hypertrophic growth (Iemitsu et al., 2001). One characteristic shift occurs in gene programs involved in cardiac fuel and energy metabolism. Mitochondrial fatty acid oxidation (FAO) genes are downregulated in pathologic cardiac hypertrophy consistent with a shift from FAO to glucose utilization for ATP synthesis in the failing heart (Allard et al., 1994; Christe and Rodgers, 1994; de las Fuentes et al., 2003; Strøm et al., 2005). This fuel shift likely serves an early compensatory role to maintain contractile function while minimizing O_2 consumption costs. Over time, ATP synthetic capacity is diminished in the pathologically hypertrophied heart. Magnetic resonance spectroscopy has shown reduced "high-energy" phosphate stores in compensated pressure overload-induced ventricular hypertrophy in animal models and humans that progressively declines during the transition to heart failure (see Ingwall and Weiss, 2004, for review). Phosphocreatine (PCr), the major phosphate pool and ATP buffer, is reduced in compensated hypertrophy prior to any decline in contractile function, suggesting a primary role in progression from compensated hypertrophy to failure (de Roos et al., 1992; Ingwall et al., 1985;

Tian et al., 1996). The [PCr]/[ATP] ratio correlates with heart failure severity and is a strong predictor of cardiovascular mortality (Neubauer et al., 1997; Neubauer, 2007). In addition, creatine kinase (CK)-mediated flux between PCr and ATP is reduced in failing human hearts (Weiss et al., 2005). Such observations support the notion that regardless of primary etiology, functional deterioration of the hypertrophied heart has an energetic basis (Ashrafian et al., 2003; Maloyan et al., 2005).

The regulatory events driving [PCr] depletion in the hypertrophied heart have not been fully elucidated. PPARγ coactivator-1α (PGC-1α) is an inducible, cardiac-enriched coactivator integrating upstream signals with transcription factors regulating cellular energy metabolism, mitochondrial respiration, and replication/transcription of the mitochondrial genome (Finck and Kelly, 2006; Lin et al., 2005). PGC-1α is upregulated in exercise-induced physiologic cardiac hypertrophy ([Wende et al., 2005]; A.R. Wende and D.P.K., unpublished data) but decreased in pathologic cardiac hypertrophy (Garnier et al., 2003; Lehman and Kelly, 2002). PGC-1α null (*PGC-1α*$^{-/-}$) mice exhibit impaired cardiac contractile responses to inotropic stimuli and to exhaustive exercise (Leone et al., 2005). An independent line of *PGC-1α*$^{-/-}$ mice develops age-dependent cardiomyopathy with reduced baseline myocardial PCr and ATP levels (Arany et al., 2005) and heart failure following prolonged pressure overload (Arany et al., 2006). In a cdk9 transgenic mouse model of heart failure, decreased mitochondrial gene expression correlated with PGC-1α protein and activity levels, and myocyte apoptosis was rescued by PGC-1α overexpression in this model (Sano et al., 2004). Thus, maximal PGC-1α activity may be required to maintain cardiac energetic capacity in the context of prolonged pathologic stress to prevent cardiac remodeling that leads to heart failure.

Despite evidence that PGC-1α contributes to the adaptive response during cardiac hypertrophic growth, little is known about relevant downstream pathways. PGC-1α coactivates a cascade of transcription factors (Finck and Kelly, 2006; Huss and Kelly, 2005). Recently, the estrogen-related receptor α (ERRα) was identified as a PGC-1α transcriptional partner (Huss et al., 2002; Schreiber et al., 2003). Subsequent studies revealed the central role of the ERRα/PGC-1α complex in regulating oxidative energy metabolism. ERRα is dependent on PGC-1α to activate transcription in oxidative tissues, such as heart and slow-twitch skeletal muscle, targeting genes involved in mitochondrial FAO and other mitochondrial pathways (Huss et al., 2004; Wende et al., 2005). Likewise, inhibiting ERRα function with siRNA knockdown or inverse agonists impairs induction of mitochondrial gene expression and respiration by PGC-1α (Mootha et al., 2004; Schreiber et al., 2004). ERRα also upregulates expression of transcription factors downstream of PGC-1α, including PPARα and nuclear respiratory factor-2 (NRF-2) (Huss et al., 2004; Mootha et al., 2004). The present study evaluates the functional and energetic response of ERRα null mice (*ERRα*$^{-/-}$) to cardiac pressure overload. Loss of ERRα predisposes to stress-induced depletion of high-energy phosphate reserves and pathologic cardiac remodeling, demonstrating the importance of the ERRα/PGC-1α pathway in myocardial adaptation to pathophysiological stress.

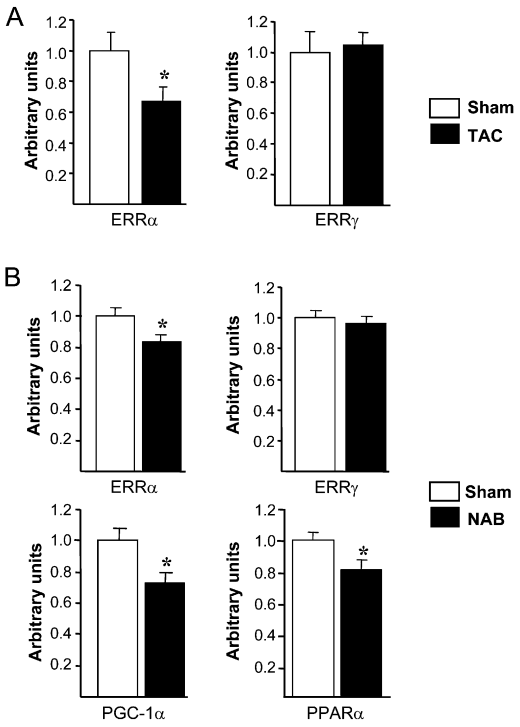

Figure 1. Expression of ERRα and Related Transcriptional Regulators of Cardiac Metabolism in Response to Pressure Overload

Real-time PCR analysis of transcript expression in WT hearts subjected to (A) 7d TAC (sham, n = 9; TAC, n = 10) or (B) neonatal arotic banding (NAB) (sham, NAB, n = 14) procedures. Data represent mean arbitrary units (±SE) normalized to WT, sham values (= 1.0). Asterisks (*) indicate significant difference ($p < 0.05$) between sham and pressure overload groups.

RESULTS

ERRα and PGC-1α Are Downregulated in Pathologic Hypertrophy

Expression of ERR isoforms and related pathways downstream of PGC-1α was assessed in response to pressure overload to investigate their potential role in pathologic hypertrophy. Transcript levels were measured in LV of wild-type (WT) mice subjected to transverse aortic constriction (TAC) or to a sham procedure (Figure 1A). ERRα transcript levels were decreased 33% in hypertrophied hearts 7d post-TAC. In contrast, no changes were observed for other transcription factors within the PGC-1α cascade, including ERRγ, PPARα, PPARβ, NRF-2a, or PGC-1α itself (Figure 1A and Table 2). Expression was then examined in a chronic neonatal aortic banding (NAB) model in which hypertrophic growth progresses over an 8wk period. While PPARα (−19%) and PGC-1α (−27%) were coordinately downregulated with ERRα (−17%) by

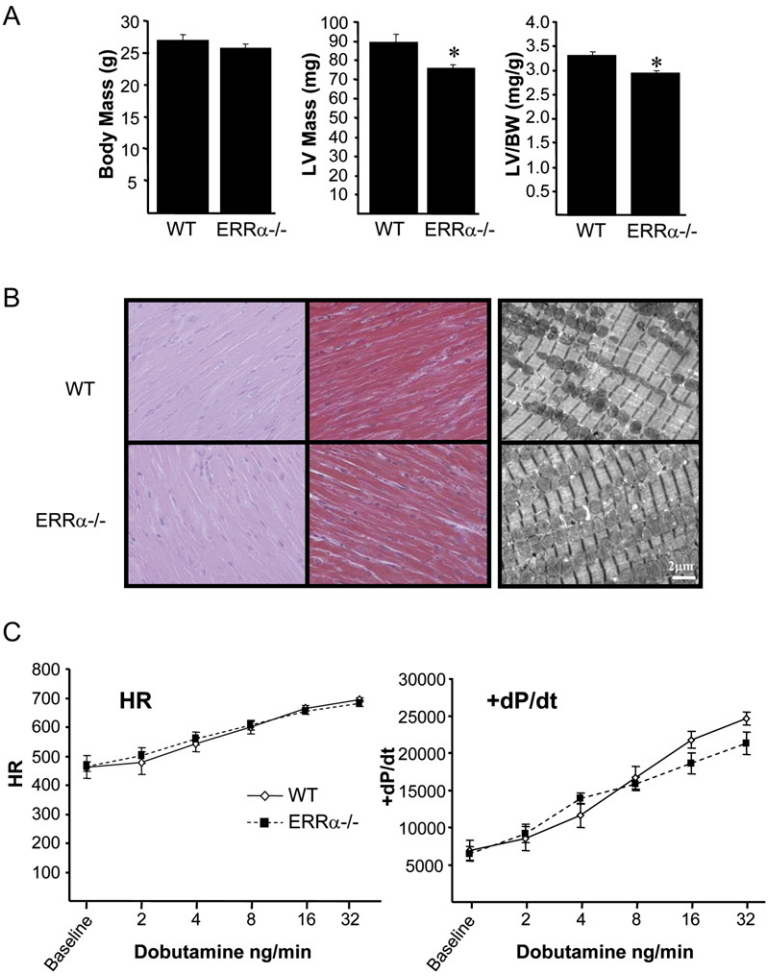

Figure 2. *ERRα*$^{-/-}$ Hearts Are Smaller with Normal Function and Histology

(A) (Left) Body weight (g) of WT (n = 21) and *ERRα*$^{-/-}$ (n = 22) mice. (middle) Absolute LV mass (mg) and (right) LV mass index, LV mass/BW (WT, n = 14; *ERRα*$^{-/-}$, n = 18). Bars represent mean (±SE) and asterisks indicate significant difference ($p < .005$) between WT and *ERRα*$^{-/-}$.

(B) Ventricular myocardium of WT and *ERRα*$^{-/-}$ hearts stained with H&E or Trichrome. Electron microscopic analysis of sarcomeric and mitochondrial ultrastructure.

(C) Hemodynamic parameters in WT (n = 5) and *ERRα*$^{-/-}$ (n = 4) mice. Heart rate and rate of systolic pressure development (+dP/dt) measured at baseline and with dobutamine administration (ng/min).

NAB; similar to the results with TAC, ERRγ expression was unaffected (Figure 1B). Thus, ERRα expression is decreased early in pathologic cardiac hypertrophy with later downregulation of PGC-1α and other cascade components.

ERRα$^{-/-}$ Hearts Exhibit a Growth Defect with Preserved Contractile Function

ERRα$^{-/-}$ mice exhibit modest baseline phenotypic abnormalities, including altered oxidative fatty acid catabolism in white adipose and reduced intestinal lipid absorption (Carrier et al., 2004; Luo et al., 2003). Recently, a defect in cold-induced thermogenesis has been described in *ERRα*$^{-/-}$ mice and attributed to deficient mitochondrial capacity in brown adipose (Villena et al., 2007). Initial characterization demonstrated that *ERRα*$^{-/-}$ hearts are smaller with lower LV mass (−15.5%) and normalized LV/BW ratio (−11%) than WT littermates (Figure 2A). Light microscopic and ultrastructural examination revealed normal myofibrillar and mitochondrial architecture in *ERRα*$^{-/-}$ hearts with no apparent change in mitochondrial number or size (Figure 2B).

Echocardiographic analysis revealed no functional differences between *ERRα*$^{-/-}$ and WT mice (Table S1). To assess contractility, hemodynamics were measured in vivo at baseline and following infusion of the β-adrenergic agonist, dobutamine. Heart rate, peak LV pressures, and rates of pressure development and relaxation (±dP/dt) were indistinguishable between WT and *ERRα*$^{-/-}$ hearts at baseline and following dobutamine challenge (Figure 2C and data not shown). Thus, ERRα deficiency results in a modest growth defect with normal contractile function.

Pathologic Remodeling of *ERRα*$^{-/-}$ Hearts in Response to Pressure Overload

The increased workload imposed by chronic pressure overload increases energetic demand. Given the hypothesis that ERRα plays a prominent role in regulating cardiac energy metabolism, we predicted that ERRα is essential for myocardial adaptation during hypertrophic growth. To test this hypothesis, adult WT and *ERRα*$^{-/-}$ animals were subjected to a 7d TAC protocol. Both groups exhibited a significant increase in LV mass indexed to body weight (Figure 3A) or tibia length (data not shown). Consistent with the hypertrophic response, pressure gradients achieved across the aortic constriction measured by Doppler velocity indicated that a significant gradient was

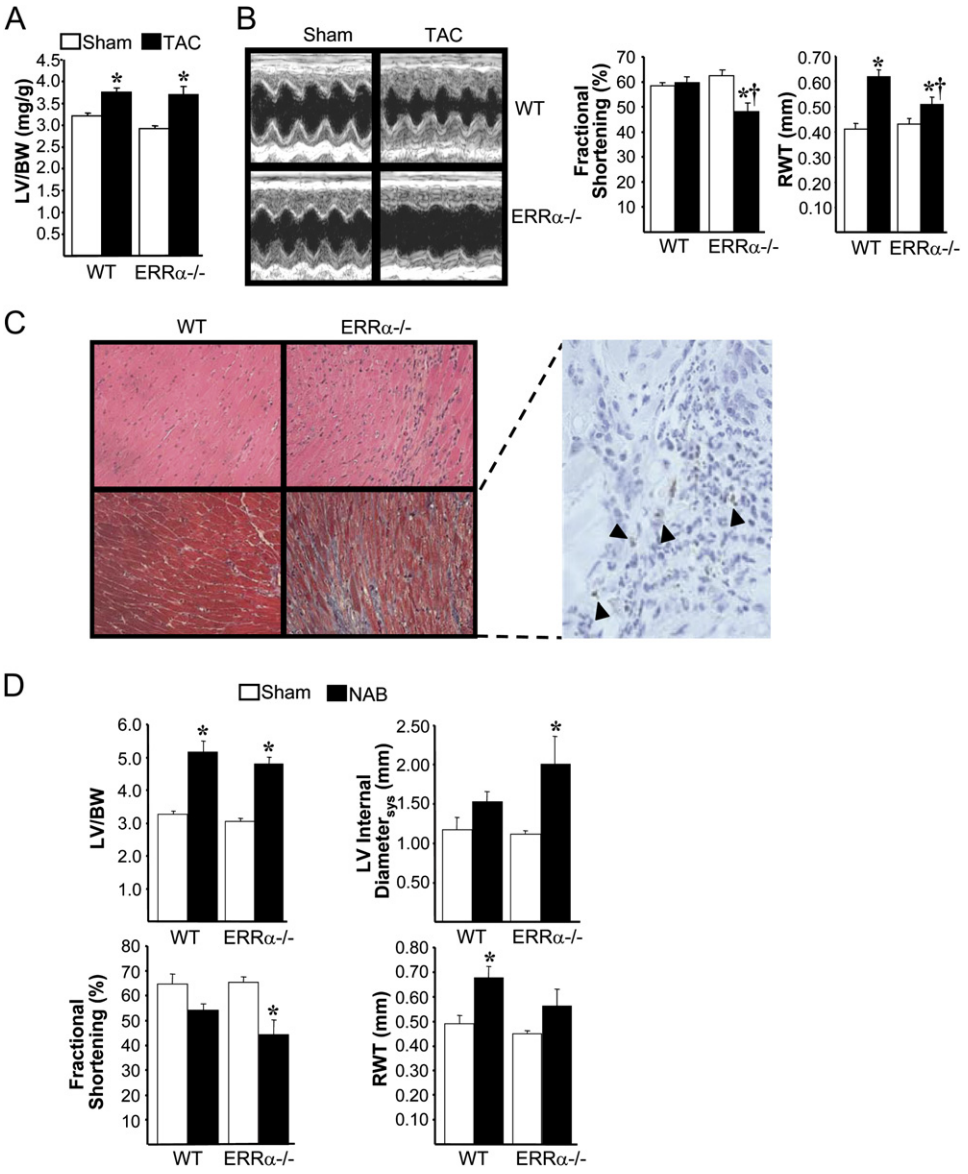

Figure 3. *ERRα*$^{-/-}$ Hearts Undergo Pathologic Ventricular Remodeling in Response to Seven Day or Chronic Pressure Overload

(A) LV mass index in WT (sham, n = 9; TAC, n = 10) and *ERRα*$^{-/-}$ (sham, n = 10; TAC, n = 12) mice. Data are reported as in Figure 2A.

(B) (left) M-mode echocardiographic (Echo) images from WT and *ERRα*$^{-/-}$ mice subjected to sham or TAC. Echo-derived LV dimensions and functional parameters: percent LV fractional shortening and relative wall thickness (RWT). Asterisks (*) indicate significant difference ($p \leq 0.05$) between sham and TAC groups for a given genotype; daggers (†) denote significant difference ($p \leq 0.05$) between genotypes within a treatment group.

(C) H&E and Trichrome staining of ventricular myocardium from TAC animals. (inset) TUNEL staining (arrowheads denote positively stained cells).

(D) LV mass index in 8wk post-NAB WT (sham, n = 6; NAB, n = 5) and *ERRα*$^{-/-}$ (sham, n = 4; NAB, n = 7) mice. Asterisks indicate significant mean differences ($p < .0005$). Echo-derived parameters measured 8 week post-NAB: LV internal systolic chamber diameter, fractional shortening, and RWT. Asterisks (*) indicate significant mean differences ($p \leq 0.05$) between sham versus NAB.

achieved in all animals (Table S1 in the Supplemental Data available with this article online). The response to TAC in *ERRα*$^{-/-}$ hearts was greater than that of WT animals such that final mean LV weights were similar between the two groups (Figure 3A) despite a slightly higher mean pressure gradient achieved in the WT mice (Table S1). In contrast to WT mice, which developed stable hypertrophy without LV dilatation or systolic dysfunction, *ERRα*$^{-/-}$ mice exhibited echocardiographic characteristics of early heart failure post-TAC. Specifically, mean LV fractional shortening (FS) was significantly reduced in *ERRα*$^{-/-}$ hearts subjected to TAC (WT, 62.6 ± 2.2%; *ERRα*$^{-/-}$, 48.0 ± 3.6%; $p \leq 0.05$; Figure 3B; Table S1). LV systolic diameter increased significantly in *ERRα*$^{-/-}$ mice post-TAC compared to sham controls or to WT mice post-TAC. In addition, relative wall thickness (RWT) increased in WT TAC mice, a normal

adaptive response to pressure overload; whereas RWT was unchanged in the *ERRα*$^{-/-}$ TAC hearts, indicating wall thinning (Figure 3B; Table S1). Consistently, fibrosis and apoptotic cell death were only observed in *ERRα*$^{-/-}$ TAC hearts (Figure 3C).

Short-term TAC does not provide information about LV remodeling in response to progressive chronic ventricular pressure overload; therefore, mice were subjected to the NAB protocol. Wt and *ERRα*$^{-/-}$ hearts exhibited dramatic hypertrophic growth (>50% increase) with NAB compared to sham controls (Figure 3D). Equivalent pressure gradients developed in both groups (data not shown). Consistent with the pathologic remodeling observed in response to TAC, only *ERRα*$^{-/-}$ hearts dilated and developed LV systolic dysfunction, indicated by diminished %FS and increased LV systolic chamber diameter (Figure 3D).

Reduced High-Energy Phosphate Reserve and ATP Synthetic Capacity in *ERRα*$^{-/-}$ Hearts

To investigate the basis for contractile failure in *ERRα*$^{-/-}$ mice caused by pressure overload, we evaluated energetic parameters in *ERRα*$^{-/-}$ hearts. Analysis of ultrastructure in ventricular samples of *ERRα*$^{-/-}$ hearts post-NAB revealed no overt mitochondrial pathology compared to WT hearts (data not shown). ^{31}P-NMR spectroscopy was used to measure myocardial phosphocreatine (PCr) and ATP levels in isolated perfused WT and *ERRα*$^{-/-}$ hearts. Baseline [PCr]/[ATP] ratios were equivalent in WT (1.6 ± 0.1) and *ERRα*$^{-/-}$ (1.5 ± 0.1) hearts (Figure 4A). As expected, contractile parameters measured concurrently with the spectroscopic analysis, were also normal in *ERRα*$^{-/-}$ hearts (Figure 4B).

The stress of TAC and NAB unveiled a contractile phenotype in *ERRα*$^{-/-}$ mice. Thus, to determine whether the functional response of *ERRα*$^{-/-}$ hearts reflected a latent energetic defect, myocardial [PCr] and [ATP] and contractile function were simultaneously measured in isolated WT and *ERRα*$^{-/-}$ hearts following increased work induced by β-adrenergic infusion. Wt and *ERRα*$^{-/-}$ hearts responded to isoproterenol similarly with an appropriate increase in heart rate, LV developed pressure (LVDP), and ± dP/dt (Figure 4B). [ATP] was unchanged during β-agonist infusion in both WT and *ERRα*$^{-/-}$ hearts (Figure 4C). However, [PCr] was depleted to a greater extent in *ERRα*$^{-/-}$ hearts compared to WT at 1 nM (WT, 91.8 ± 5.2%; *ERRα*$^{-/-}$, 66.2 ± 5.7%; $p \leq 0.01$) and 5 mM (WT, 73.7 ± 6.3%; *ERRα*$^{-/-}$, 50.5 ± 6.5%; $p \leq 0.03$) isoproterenol (Figure 4C).

Subsequently, hearts were subjected to 15 min of no-flow ischemia followed by 40 min of aerobic reperfusion (I/R). The ischemic period depletes PCr and ATP stores, so rates of depletion and functional recovery can be assessed. During the ischemic phase, despite WT and *ERRα*$^{-/-}$ hearts having equivalent initial [ATP], the rate of [ATP] depletion in *ERRα*$^{-/-}$ hearts was more rapid than in controls (Figure 4D). During the 40 min reperfusion period, when oxidative ATP production is re-initiated, [PCr] recovery rate was slower during the early reflow period (10 and 20 min) for *ERRα*$^{-/-}$ compared to WT hearts, which exhibited a commonly observed [PCr] overshoot (>100% of pre-ischemic levels) at these time points, though by the end of reperfusion (40 min) [PCr] had normalized between the two groups (Figure 4E). In contrast, [ATP] was equivalent at the 10 and 20 min reflow time points, but reduced in *ERRα*$^{-/-}$ hearts compared to WT at the end of reperfusion. Correlating with reduced [ATP], recovery of contractile parameters, rate pressure product (RPP) and LVDP, was impaired in *ERRα*$^{-/-}$ hearts (Figure 4F). Collectively, the reduced capacity for [PCr] and [ATP] repletion in response to energetic stress is consistent with defects in ATP synthesis in *ERRα*$^{-/-}$ hearts, and the resulting decrease in ventricular performance is a consequence of depleted ATP pools.

To further assess ATP synthetic capacity of *ERRα*$^{-/-}$ hearts, mitochondrial respiratory function and ATP synthesis rates were assessed in endocardial strips prepared from WT and *ERRα*$^{-/-}$ mice. Measurement of O_2 consumption using palmitoylcarnitine (PC) or pyruvate (Figure 4G) as substrates revealed that basal (-ADP) and State 3 (+ADP, maximally stimulated) rates were not different between the groups. In contrast, the ATP synthesis rate normalized to O_2 consumption (ATP/O) in *ERRα*$^{-/-}$ cardiac strips was reduced with both PC (~49.6%) and pyruvate (~38.6%) compared to WT tissue (Figure 4H).

Pathologic Cardiac Remodeling in *ERRα*$^{-/-}$ Mice Correlates with Altered Expression of Genes Involved in ATP Synthesis and High-Energy Phosphate Transfer

To delineate ERRα target pathways involved in the bioenergetic and functional abnormalities in *ERRα*$^{-/-}$ hearts microarray analyses were performed to characterize gene expression changes in these hearts. The number of metabolic genes downregulated was relatively low, consistent with the absence of functional baseline abnormalities in the *ERRα*$^{-/-}$ hearts. However, expression of genes involved in multiple energy metabolic pathways was altered in *ERRα*$^{-/-}$ hearts including fatty acid uptake and oxidation (fatty acyl-CoA synthase, CD36/fatty acid transporter, acyl-CoA oxidase); TCA cycle (isocitrate dehydrogenase 2); ETC/Oxphos (NADH dehydrogenase 1b3, cytochrome oxidase subunit VIIIb, ATP synthase 5e); and ATP phosphate transfer (mitochondrial creatine kinase 2) (Table 1). Many of these genes were previously identified as candidate ERRα targets in gain-of-function studies performed by our group and others (Huss et al., 2004; Mootha et al., 2004; Schreiber et al., 2004). A second strategy, employing ERRα chromatin immunoprecipitation coupled to promoter arrays (ChIP-chip) further informed our selection of putative ERRα target genes for validation by real-time PCR. These latter studies are described in detail in an independent report (Dufour et al., 2007).

The complementary unbiased approaches identified overlapping candidate energy metabolic pathways relevant to the *ERRα*$^{-/-}$ cardiac phenotype. Importantly, ERRα target genes involved in ATP synthesis and high-energy phosphate transfer were identified. Expression of these genes was evaluated using real-time PCR in all

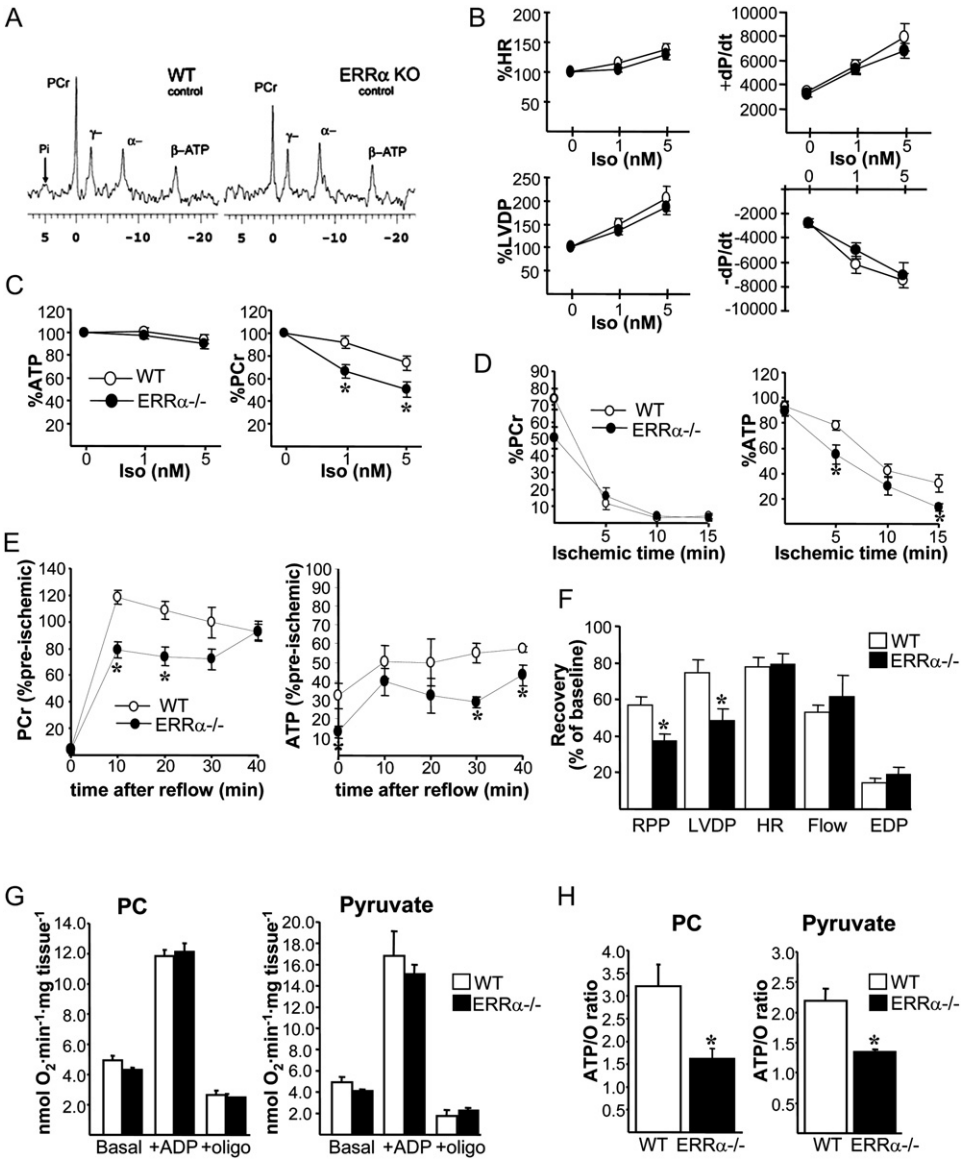

Figure 4. Defects in Cardiac Energetics in *ERRα*$^{-/-}$ Mice

(A) ^{31}P-NMR baseline spectra, showing peaks for PCr, ATP phosphates (α, β, γ) and free phosphate (P_i).

(B–E) (B) Hemodynamics and (C) PCr and ATP levels measured at baseline and after 1 nM and 5 nM isoproterenol (Iso) administration. Measurements of PCr and ATP during (D) ischemia and (E) following reperfusion.

(F) Recovery of contractile function after reperfusion. RPP, rate pressure product; LVDP, left ventricular developed pressure; EDP, end-diastolic pressure. Data represent mean percent measurements (±SE) relative to baseline values (set to 100%), and asterisks (*) indicate significant difference ($p < 0.05$) between WT and *ERRα*$^{-/-}$ (n = 7).

(G) Mitochondrial respiration in WT or *ERRα*$^{-/-}$ endocardial strips using palmitoylcarnitine (PC) or pyruvate as substrates. O_2 was measured at basal state, maximal (+ADP), and plus oligomycin (+oligo).

(H) ATP synthesis rates measured with PC (left) or pyruvate (right) as respiration substrates. Asterisks (*) indicate significant difference ($p < 0.05$) between WT (n = 8) and *ERRα*$^{-/-}$ (n = 10) hearts.

four treatment groups (WT/sham, WT/TAC, *ERRα*$^{-/-}$/sham, *ERRα*$^{-/-}$/TAC; Table 2). Genes involved in ATP synthesis were dysregulated in a pattern consistent with the metabolic and functional derangements observed in *ERRα*$^{-/-}$ hearts at baseline or in response to TAC. Specifically, ETC genes encoding subunits of Complex I (Ndufs3), Complex II (SDHA), the electron transferring flavoprotein complex (Etfa and Etfd), and cytochrome c were all significantly downregulated in *ERRα*$^{-/-}$/TAC but not in the sham groups (Figure 5A, Table 2). This regulatory pattern strongly suggested a link to the cardiac functional phenotype; given that contractile dysfunction in the *ERRα*$^{-/-}$ hearts was unveiled with pressure overload, when demands for ATP synthesis increase. In addition,

Table 1. Decreased Metabolic Genes in *ERRα*$^{-/-}$ Hearts by Microarray Analysis

Accession	Gene Symbol	Gene Name
Lipid Metabolism		
U15977	*Acsl1*	Fatty acyl-CoA synthetase, long chain
L23108	*Cd36*	CD36, fatty acid transporter
AF006688	*Acox1*	Acyl-CoA oxidase
Tricarboxylic Acid Cycle		
U51167	*Idh2*	Isocitrate dehydrogenase 2
Electron Transport / Oxidative Metabolism		
NM_025597	*Ndufb3*	NADH dehydrogenase (ubiquinone) 1 beta subcomplex 3
AV260484	*Cox8b*	Cytochrome c oxidase subunit VIIIb
NM_025983	*Atp5e*	ATP synthase H^+ transporting, F1 complex, epsilon subunit
NM_198415	*Ckmt2*	Creatine kinase, mito 2 (sarcomeric)
Other Metabolic Processes		
NM_024255	*Hsdl2*	Hydroxysteroid dehydrogenase like 2
XM_128781	*Lycat*	Lysocardiolipin acyltransferase
Purine Nucleotide Metabolism		
M74495	*Adss*	Adenylosuccinate synthetase
X68193	*Nme2*	Nucleoside diphosphate kinase B

two genes encoding enzymes functionally coupled to the ATP synthase complex, mitochondrial creatine kinase 2 (mtCK2) and adenine nucleotide translocator 1 (ANT1), were downregulated in *ERRα*$^{-/-}$ hearts at baseline and following TAC (Figure 5A, Tables 1 and 2). ANT1 and mtCK2 coordinate phosphate transfer from nascent ATP to creatine with the shuttling of regenerated ADP back into the mitochondrial matrix (Saks et al., 2004). The related mtCK1 and CK-B genes were upregulated, suggesting a switch in CK isoforms in *ERRα*$^{-/-}$ hearts. Additional genes involved in cardiac fuel utilization pathways, including FAO (VLCAD) and glucose uptake (GLUT4), were also downregulated in *ERRα*$^{-/-}$ hearts (Figure 5A, Table 2). The FAO gene MCAD was decreased only with the development of dysfunction post-TAC. Collectively, these analyses define potential ERRα targets and implicate causal role for genes involved in ATP and PCr homeostasis in the cardiac phenotype of *ERRα*$^{-/-}$ mice.

Protein levels were assessed for a subset of the metabolic targets and showed a similar pattern as the transcripts, but with lower magnitude changes. Ndufs3 and cyt c protein expression was lower in the *ERRα*$^{-/-}$ hearts (Figure 5C). Interestingly, cyt c protein was reduced in sham and TAC *ERRα*$^{-/-}$ hearts, whereas its transcript was downregulated only in the TAC group (Figure 5C). Levels of F_1-ATPase subunit were decreased in *ERRα*$^{-/-}$/TAC hearts only; and VDAC1, involved in ATP translocation, was reduced in sham and TAC *ERRα*$^{-/-}$ hearts. Taken together, the expression analyses suggest that reduced expression of energy metabolic genes at baseline, as well as in response to pressure overload, contributes to the observed contractile failure in the *ERRα*$^{-/-}$ hearts.

A subset of ERRα target genes were downregulated only following imposition of pressure overload (Figure 5A, Table 2), suggesting that compensatory regulation present under basal conditions, were deactivated during cardiac hypertrophic growth. To explore this possibility, the expression of several key transcription factors known to share target genes with ERRα, including PGC-1, ERRγ, and NRF isoforms was assessed. Expression of ERRγ, PGC-1α, and Gabpa (NRF-2a) was increased in sham *ERRα*$^{-/-}$ hearts, an effect that was reversed following TAC (Figure 5B, Table 2). These results suggest that compensatory mechanisms maintain bioenergetic capacity in unstressed *ERRα*$^{-/-}$ hearts, but following pressure overload, a stimulus known to downregulate the PGC-1α regulatory circuit (Figure 1), this mechanism is deactivated.

DISCUSSION

The healthy adult heart has remarkable ATP synthetic capacity and energetic reserve, matching oxidative ATP synthesis with cardiac work. In response to chronic pathophysiologic loads, as occurs with hypertension, the hypertrophied heart ultimately decompensates and fails. Recent evidence implicates derangements in myocardial bioenergetics in the transition from stable cardiac hypertrophy to heart failure (Allard et al., 1994; Christe and Rodgers, 1994; de las Fuentes et al., 2003; Ingwall and Weiss, 2004; Sack et al., 1997; Strøm et al., 2005; Ye et al., 2001). The role of bioenergetic abnormalities as a primary event in heart failure progression and the gene regulatory pathways governing this metabolic "reprogramming" have not been fully delineated. Herein, we

Table 2. Gene Expression Analysis by Real-time PCR in WT and *ERRα*$^{-/-}$ Hearts at Baseline and Subjected to Seven Day TAC

	WT		KO	
Common Name (Gene Symbol)	Sham	TAC	Sham	TAC
Lipid Metabolism				
Medium-chain acyl-CoA dehydrogenase (*Acadm*)	1.0 (.08)	0.78 (.09)	0.82 (.1)	0.44 (.03)[a,b]
Very long-chain acyl-CoA dehydrogenase (*Acadvl*)	1.0 (.18)	0.86 (.06)	0.60 (.08)[b]	0.48 (.04)
Carnitine palmitoyltransferase 1b, muscle (*Cpt1b*)	1.0 (.14)	1.16 (.07)	1.15 (.07)	1.05 (.13)
Acyl-CoA oxidase (*Acox1*)	1.0 (.11)	0.81 (.09)	0.79 (.07)	0.69 (.06)
CD36/fatty acid transporter (*Cd36*)	1.0 (.12)	0.65 (.09)[a]	0.76 (.06)	0.57 (.07)
Carbohydrate Metabolism				
GLUT1, glucose transporter 1, (*Slc2a1*)	1.0 (.06)	1.0 (.10)	1.35 (.12)[b]	1.35 (.16)[b]
GLUT4, glucose transporter 4, (*Slc2a4*)	1.0 (.19)	0.49 (.06)[a]	0.40 (.08)[b]	0.32 (.08)
Hexokinase 2 (*Hk2*)	1.0 (.07)	0.86 (.10)	1.02 (.14)	0.65 (.04)[a]
Electron Transport/Oxidative Metabolism				
NADH dehydrogenase (ubiq.) 1b3 (*Ndufb3*)	1.0 (.07)	0.92 (.08)	1.03 (.10)	0.64 (.06)[a,b]
NADH dehydrogenase (ubiq.) 1b7 (*Ndufb7*)	1.0 (.11)	0.82 (.04)	0.83 (.06)	0.62 (.03)
NADH dehydrogenase (ubiq.) Fe-S protein 3 (*Ndufs3*)	1.0 (.09)	0.77 (.05)	1.05 (.06)	0.56 (.05)[a]
Succinate dehydrogenase subunit A (*Sdha*)	1.0 (.10)	0.97 (.10)	1.28 (.06)	0.80 (.06)[a]
Succinate dehydrogenase subunit B (*Sdhb*)	1.0 (.12)	0.82 (.08)	1.66 (.21)[b]	1.11 (.16)
Electron transferring flavoprotein, alpha (*Etfa*)	1.0 (.04)	0.80 (.08)	1.22 (.11)	0.68 (.07)[a]
Electron transferring flavoprotein, dehydrogenase (*Etfdh*)	1.0 (.11)	0.89 (.11)	1.74 (.34)	0.88 (.08)[a]
Cytochrome c (*Cycs*)	1.0 (.16)	1.19 (.13)	1.08 (.17)	0.64 (.09)[b]
Cytochrome c oxidase, subunit II (*Cox2*)	1.0 (.16)	1.03 (.1)	0.91 (.14)	0.91 (.16)
Cytochrome c oxidase, subunit IV isoform 1 (*Cox4i1*)	1.0 (.04)	0.95 (.03)	0.82 (.03)[b]	0.79 (.04)[b]
ATP synthase, H^+ transporting F1 complex., beta (*Atp5b*)	1.0 (.12)	0.87 (.07)	0.95 (.1)	0.82 (.08)
Uncoupling protein 3 (*Ucp3*)	1.0 (.18)	0.50 (.1)	1.13 (.12)	1.50 (.42)[b]
Energy Transfer				
Creatine kinase, mitochondrial 1, ubiquitous, (*Ckmt1*)	1.0 (.15)	0.96 (.12)	3.17 (.40)[b]	6.17 (1.65)[a,b]
Creatine kinase, mitochondrial 2, sarcomeric, (*Ckmt2*)	1.0 (.09)	0.68 (.08)[a]	0.78 (.06)	0.47 (.03)[a]
Creatine kinase, brain (*Ckb*)	1.0 (.08)	1.10 (.07)	1.55 (.17)[b]	1.59 (.09)[b]
Creatine kinase, muscle (*Ckm*)	1.0 (.05)	0.81 (.03)	0.93 (.09)	0.97 (.09)
Adenine nucleotide translocator 1 (*Slc25a4*)	1.0 (.13)	0.59 (.04)[a]	0.68 (.05)[b]	0.52 (.06)
Muscle Contraction and Hypertrophic Markers				
Natriuretic peptide, type A (*Nppa*)	1.0 (.16)	4.57 (.88)[a]	3.02 (.47)	10.57 (1.94)[a,b]
Natriuretic peptide, type B (*Nppb*)	1.0 (.14)	2.75 (.59)[a]	1.13 (.23)	1.46 (.17)
β-myosin heavy chain (*Myh7*)	1.0 (.06)	4.13 (0.95)[a]	1.89 (.48)	2.87 (.34)
α-myosin heavy chain (*Myh6*)	1.0 (.09)	0.90 (.08)	0.98 (.09)	0.95 (.06)
ATPase, Ca^{2+}-transporting, cardiac, Serca2a (*Atp2a2*)	1.0 (.15)	0.95 (.06)	0.87 (.13)	0.74 (.10)
Transcriptional Regulation				
ERRγ (*Esrrg*)	1.0 (.11)	1.08 (.09)	1.57 (.03)[b]	1.08 (.09)[a]
PGC-1α (*Ppargc1a*)	1.0 (.13)	1.15 (.09)	2.50 (.63)[b]	1.18 (.25)[a]
NRF-1, nuclear respiratory factor-1 (*Nrf1*)	1.0 (.08)	1.0 (.09)	1.66 (.13)[b]	1.72 (.13)[b]
Gabpa/NRF-2a, GA repeat binding protein, alpha (*Gabpa*)	1.0 (.11)	0.73 (.07)	1.52 (.13)[b]	0.91 (.08)[a]
mtTFA, transcription factor A, mitochondrial (*Tfam*)	1.0 (.09)	0.90 (.11)	0.78 (.06)	0.67 (.06)

Table 2. *Continued*

Common Name (Gene Symbol)	WT		KO	
	Sham	TAC	Sham	TAC
PPARα (*Ppara*)	1.0 (.06)	1.0 (.07)	0.60 (.07)[b]	0.50 (.05)[b]
PPARβ (*Ppard*)	1.0 (.16)	1.12 (.11)	1.20 (.08)	0.95 (.12)

[a] Sham versus TAC, $p \leq 0.05$.
[b] WT versus KO, $p \leq 0.05$, n = 7 for all groups.

demonstrate that expression of the *ERRα* gene is downregulated in the pathologically hypertrophied heart. Moreover, we found that deletion of the *ERRα* gene in mice accelerates the bioenergetic and functional signatures of heart failure in the context of pressure overload. These results are important because ERRα, as a critical component of the PGC-1α gene regulatory cascade, regulates the transcription of genes involved in mitochondrial energy metabolism. These findings are consistent with independent microarray datasets demonstrating ERRα downregulation in pathologic cardiac hypertrophy in mice and heart failure in humans (Gene Expression Omnibus [GEO] database [Barrett et al., 2007]; GEO series accession: GSE76; GSE1145).

Reduced high-energy phosphate stores ([PCr]), a metabolic signature of pathologic cardiac hypertrophy and heart failure, results from a mismatch in ATP supply and demand (Ingwall and Weiss, 2004; Neubauer, 2007). Potential mechanisms responsible for depletion of energy stores include defects in ATP synthesis, alterations in mitochondrial ADP-ATP translocation, reduction in myocardial substrate flux, and constraints on high-energy phosphate transfer due to altered creatine kinase (CK) activity. ATP flux through CK is reduced in humans with mild heart failure

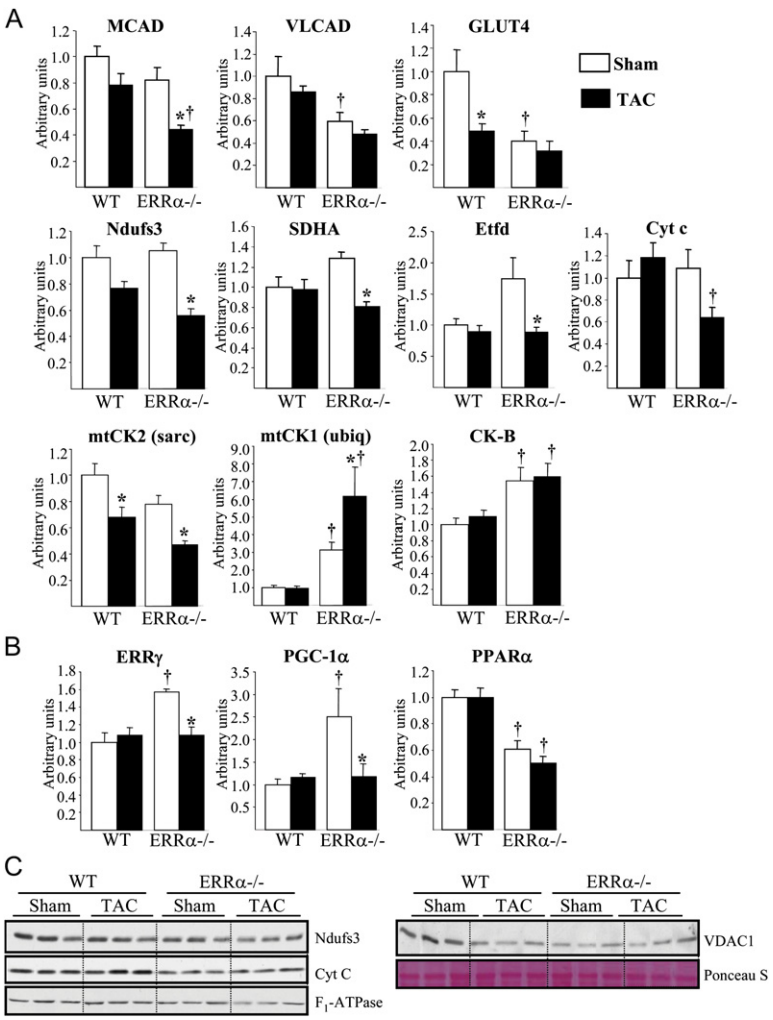

Figure 5. Decreased Expression of Genes Involved in Cardiac Energy Metabolism in *ERRα*$^{-/-}$ Hearts

Real-time PCR expression analysis of genes encoding (A) enzymes involved in energy metabolism or (B) regulatory proteins was assessed. Fatty acid and glucose utilization: medium- and very long-chain acyl-CoA dehydrogenase (MCAD, VLCAD), glucose transporter 4 (GLUT4); ETC/Oxphos targets: NADH dehydrogenase (ubiquinone) Fe-S protein 3 (Ndufs3); succinate dehydrogenase subunit A (SDHA); electron transferring flavoprotein dehydrogenase (Etfd); and cytochrome c (Cyt c); Phosphate transfer: mitochondrial creatine kinase 2 (mtCK2, sarcomeric), mtCK1 (ubiquitous) and cytosolic brain-type CK (CK-B); (B) Transcription factors: ERRγ, PGC-1α and PPARα. Data represent mean arbitrary units (±SE) normalized to WT, sham values (= 1.0). Asterisks (*) indicate significant difference ($p \leq 0.05$) between sham and TAC groups for a given genotype; daggers (†) denote significant difference ($p \leq 0.05$) between genotypes within a treatment group (all groups, n = 7). (C) Immunoblot analysis of extracts from WT or *ERRα*$^{-/-}$ hearts subjected to sham or TAC. Representative subunit proteins from the ETC/Oxphos complexes were analyzed. Voltage-dependent anion channel 1 (VDAC 1/porin).

(Weiss et al., 2005), resulting in loss of ATP buffering capacity and increased direct reliance on mitochondrial ATP synthesis which could limit the response to acute and chronic increases in contractile demand. The importance of efficient, high capacity, mitochondrial ATP synthesis is underscored by the cardiomyopathy phenotype associated with genetic defects in these pathways (Palmieri et al., 2005; Wallace, 2000).

Genetic defects in mitochondrial FAO, the key fuel source for myocardial ATP synthesis, cause cardiomyopathy in humans (Bennett et al., 2000; Kelly and Strauss, 1994). Abnormalities in glucose metabolism are also associated with cardiac dysfunction in animal models. Disruption of the insulin sensitive glucose transporter, GLUT4, leads to cardiac hypertrophy and enhanced ischemia-reperfusion injury (Tian and Abel, 2001; Weiss et al., 2002). Our results indicate that whereas contractile function is normal at baseline, *ERRα*$^{-/-}$ mouse hearts exhibit decreased [PCr]/[ATP] and impaired PCr and ATP recovery in response to adrenergic and ischemia-reperfusion stress, respectively. Although not a direct measure of ATP synthetic capacity, [PCR]/[ATP] is an index of cellular energetics (Ingwall and Weiss, 2004; Neubauer, 2007). Consistent with recent evidence that ERRα regulates multiple pathways of cardiac mitochondrial energy metabolism, we found that genes involved in FA and glucose oxidation, TCA, ETC/Oxphos, and phosphate transfer are perturbed in *ERRα*$^{-/-}$ hearts at baseline and, in some cases, to a greater degree following pressure overload. These data support the conclusion that depletion of PCr stores seen in *ERRα*$^{-/-}$ hearts reflects underlying bioenergetic defects related to reduced expression of genes downstream of PGC-1α/ERRα. In further support of this conclusion, respiration studies demonstrated that the ATP synthesis/O_2 consumption ratio is reduced in *ERRα*$^{-/-}$ hearts. We conclude that following pressure overload, ERRα-deficient mice develop contractile dysfunction due to abnormalities in both ATP synthesis and high-energy phosphate transfer as occurs in human forms of heart failure.

The observed gene expression changes provide insight into the basis for abnormal cardiac energetics in *ERRα*$^{-/-}$ mice. Previous microarray studies in cardiac myocytes overexpressing ERRα identified potential target genes involved in energy substrate metabolism, including FA uptake and oxidation, glucose metabolism, and ETC/Oxphos (Huss et al., 2004). The same target genes were decreased in *ERRα*$^{-/-}$ hearts either at baseline (PPARα, acyl-CoA synthase, CD36, acyl-CoA oxidase, VLCAD, GLUT4, mtCK2, ANT1, and cytochrome oxidase subunits IV and VIII) or following TAC (MCAD, hexokinse, Etfa, Etfdh, Cyt c). Independent expression analyses support a role for ERRα as a direct transcriptional regulator of genes involved in cardiac fuel metabolism and energetics, a conclusion validated and expanded by the ChIP-chip studies. The method and complete characterization of cardiac ERRα gene targets by ChIP-chip was recently described (Dufour et al., 2007). Collectively, our gene expression results are consistent with the metabolic assessment of *ERRα*$^{-/-}$ hearts, indicating abnormalities in both ATP synthetic capacity and PCr homeostasis. We found altered expression of ERRα target genes involved in several pathways important for ATP synthesis including FAO, the TCA cycle, ETC/Oxphos, and the ATP synthesis/translocation complex. In addition, expression of the glucose transporter, GLUT4, was downregulated in the *ERRα*$^{-/-}$ hearts. Whereas GLUT4 was not shown to be a direct ERRα target in unbiased ChIP-chip studies (Dufour et al., 2007), the *ERRα*$^{-/-}$ hearts exhibit a downregulation of AMPKβ subunits, Prkab1 and Prkab2, accompanied by reduced AMPKα and ACC phosphorylation (Dufour et al., 2007). The AMPK signaling pathway is an important regulator of GLUT4 translocation and *Slc2A4* transcription (Holmes et al., 2005). Our studies also revealed evidence for abnormal expression of genes involved in high-energy phosphate transfer, including mtCK and ANT1. ATP synthetic capacity is also likely reduced due to inefficient synthesis, possibly due to uncoupling. We observed no change in UCP3 expression in *ERRα*$^{-/-}$ hearts at baseline (Table 2), though UCP3 independent uncoupling has been reported (Boudina et al., 2005). However, the expected downregulation of UCP3 gene expression in response to pressure overload (Taegtmeyer et al., 2002), did not occur in the *ERRα*$^{-/-}$/TAC hearts, possibly resulting in a relative increase in respiratory uncoupling and a reduction in ATP synthetic capacity.

PGC-1α coactivates multiple nuclear receptor and non-nuclear receptor transcription factors regulating distinct, yet overlapping, gene targets involved in cardiac energy metabolism (Huss and Kelly, 2005). This work identifies ERRα, a specific PGC-1α partner, as important for the bioenergetic and functional adaptation of the heart to hemodynamic stress imposed by pressure overload. Since ERRα regulates entire metabolic programs, the phenotype of *ERRα*$^{-/-}$ hearts cannot be ascribed to a single altered target gene, except ERRα itself. In addition, the expression pattern of PGC-1α and ERRγ in *ERRα*$^{-/-}$ hearts suggests a "compensatory" response that is inactivated during hypertrophy possibly accounting for pathologic cardiac remodeling in *ERRα*$^{-/-}$ mice. Indeed, as described in this issue of *Cell Metabolism* by Alaynick et al., the cardiac phenotype of ERRγ null hearts supports the involvement of this isoform in regulating cardiac energy metabolism (Alaynick et al., 2007). The relevance of this putative compensatory mechanism must be tested in experimental models that prevent inactivation of the PGC-1α/ERRα pathway. Such studies will help determine the therapeutic potential of targeting the ERR/PGC-1α pathway for the treatment of heart failure.

EXPERIMENTAL PROCEDURES

Animals

Adult (10–12 weeks) male WT or *ERRα*$^{-/-}$ mice were studied. Wt and *ERRα*$^{-/-}$ mice are on the hybrid C57Bl6/svJ129 strain originally characterized by the Giguère laboratory (Luo et al., 2003). The C57Bl6/svJ129 line was maintained through successive generation intercrosses and baseline characterizations were performed on WT and *ERRα*$^{-/-}$ littermates from heterozygous (*ERRα*$^{+/-}$) matings. For TAC

and NAB studies, WT or *ERRα*$^{-/-}$ mice from heterozygous matings (maintenance hybrid line) were mated to generate sufficient littermates for treatments. Although experiments were performed on hybrid mice, the pure strains (C57BL/6 or svJ129) respond similarly with maintenance of ventricular function in the TAC pressure overload model (unpublished data). Animal studies complied with NIH guidelines for humane treatment of laboratory animals and were approved by the Animal Studies Committee of Washington University.

Histology and Electron Microscopy

Midventricle slices were formalin-fixed, and paraffin-embedded sections stained with Masson's trichrome or H&E for light microscopy. For electron microscopy, LV papillary muscles were fixed in Karnovsky's fixative, postfixed in 1% OsO_4, and embedded in poly bed 812. Thin sections were stained with uranyl acetate/lead citrate.

Hemodynamic Studies

Hemodynamic studies were performed as previously described (Rockman et al., 1991). The right carotid artery of anesthetized mice (sodium thiopental, 60 mg/kg) was cannulated with a 1.4-French high fidelity micromonometer catheter (Millar Instruments), inserted into the left atrium, advanced across the mitral valve, and secured in the LV. Hemodynamic measurements were recorded at baseline and for 1 min increments following β_1-adenergic receptor agonist (dobutamine) infusions (2, 4, 8, 16, 32 ng/gBW/min). Continuous aortic pressures, LV systolic and diastolic pressures, and the derivative of LV pressure (dP/dT) were collected and digitized with BioBench data acquisition software (National Instruments).

Transverse Aortic Constriction and Neonatal Aortic Banding Protocols

Transverse aortic constriction (TAC) is an established procedure for producing LV hypertrophy (Rockman et al., 1991; Sack et al., 1997). Wt or *ERRα*$^{-/-}$ mice were anesthetized (ketamine [87 mg/kg]/xylazine [13 mg/kg]). Following aortic dissection through intercostal muscles, 7.0 silk suture was tied around the transverse aorta and a blunt 27 g needle, which was removed to introduce a tight constriction. For neonatal aortic banding (NAB), 18- to 20-day-old mice, weighing 12–15 g, received ascending aortic constrictions as described above. Seven days (TAC) or 8 weeks (NAB) postsurgery, noninvasive transthoracic echocardiograms were performed (9:00-11:00 am). Hearts were excised from mice euthanized between 1:00-3:00 pm by CO_2 inhalation, and LV was dissected for analyses.

Heart Langendorff Perfusion and ^{31}P NMR Spectroscopy

Spectroscopic analysis of hearts from untreated WT or *ERRα*$^{-/-}$ mice was performed as described (Cross et al., 2002; Imahashi et al., 2004). Hearts were excised from anesthetized mice (sodium pentobarbital [80 mg/kg]), cannulated and perfused in Langendorff mode at a constant pressure of 90cm of H_2O with phosphate-free Krebs-Heinseleit buffer (37°C, [pH 7.4]) containing (mmol/l): 120 NaCl, 11 glucose, 25 $NaHCO_3$, 1.75 $CaCl_2$, 5.9 KCl, and 1.2 $MgSO_4$. Contractile function was monitored with a latex balloon inserted into the LV and connected to a pressure transducer (Argon/Maxxim Medical) and data were acquired with PowerLab system (AD Instruments). Intracellular pH (pH_i), PCr, ATP and P_i, were continuously monitored by acquiring 5 min ^{31}P NMR spectra using a Varian Inova 500 MHz NMR spectrometer with an 11.7 Tesla superconducting magnet at the ^{31}P resonance frequency of 202.47 MHz. The pH_i was determined from chemical shift difference between PCr and intracellular P_i resonances. Perfused hearts were stabilized for 15 min while the magnet was shimmed and control NMR spectra were acquired. Isoproterenol (1nM and 5nM) was infused for 5 min periods during which contractile and NMR measurements were collected. After isoproterenol treatment, hearts were made globally ischemic for 15 min followed by 40 min reperfusion. Recovery of post-ischemic energetics and contractile function, expressed as percentage of pre-ischemic function, was assessed.

Mitochondrial Respiration Studies

Mitochondrial respiration rates were measured in saponin-permeabilized endocardial strips from WT (n = 8) and *ERRα*$^{-/-}$ (n = 9) mice as described (Saks et al., 1998). Inner endocardial layer strips were dissected from mixed endocardium/subendocardium slices initially excised from the LV. Endocardial fibers were separated along the long bundle axis, and transferred to buffer with 50 μg/ml saponin for permeabilization. Respiration assays were performed in a sealed, water-jacketed (25°C) chamber in respiration buffer containing 0.2 mM palmitoylcarnitine or 10 mM pyruvate (both with 5 mM malate) substrates as described (Saks et al., 1998). Dissolved O_2 was measured with a FOXY-AL300 fiber optic probe coupled to a USB-LS-450 LED excitation light source and USB2000 Spectophotometer (Ocean Optics) to assess basal (-ADP, non-ATP generating), State 3 maximal (+ADP); and uncoupled (+oligomycin, an ATP synthase inhibitor) respiration rates. Rates were calculated from O_2 consumption trace slopes (OOI Sensors software) and expressed as nmol O_2/min/mg tissue dry WT. For ATP measurements, 10 μl aliquots were removed from State 3 respiring strips in 10 s intervals, the chamber resealed, and O_2 consumption measured. Sample ATP content was analyzed by quantifying light emission from recombinant luciferase enzyme and Enlighten luciferin substrate (Promega). ATP concentrations were interpolated from a standard curve.

DNA Microarray

Total mouse ventricle RNA was reverse transcribed (Superscript II, Invitrogen Corp.) with T7 promoter-polyA primer (T7T24), followed by second strand synthesis, and generation of biotin-labeled cRNA as described (Huss et al., 2004). The Alvin Siteman Cancer Center's Multiplexed Gene Analysis Core at Washington University School of Medicine performed hybridization to Affymetrix mouse U74A chip. Affymetrix MAS 5.0 software was used for initial analysis and background normalization, and subsequent data analysis was performed in Excel. Probe sets called "absent" by MAS 5.0 in both WT and *ERRα*$^{-/-}$ heart samples were excluded. Signal intensities were normalized to average intensity for all probe sets and ratios were calculated as *ERRα*$^{-/-}$: WT. Two independent trials using pooled RNA from 3 WT or *ERRα*$^{-/-}$ hearts were performed. Signal intensity ratios $\leq$ 0.5 in both trials were considered as potentially downregulated targets in *ERRα*$^{-/-}$ hearts. Data have been submitted to the NCBI database (GEO series accession: GSE8106).

Quantitative Real-Time PCR and Immunoblot Analyses

Real-time PCR was performed to quantify relative cardiac transcript levels in the various treatment groups. Applied Biosystems reagents were used for reverse transcription (MultiScribe MuLV reverse transcriptase) of RNA and real-time PCR reactions (SYBR green PCR or TaqMan Universal PCR Master mixes) containing 0.4 μM gene specific primers or primers plus 0.1 μM Taqman probes (5′FAM and 3′TAMRA modified). Primer and probe sequences are provided in Table S2. PCR reactions were analyzed in triplicate on the Applied Biosystems Prism 7500. Transcript levels were normalized to 36B4 ribosomal RNA.

For immunoblot analysis 40 μg of total protein extracted from the heart apex was resolved on 9% SDS-PAGE and transferred to Protean II nitrocellulose (Schleicher & Schuell). Overnight incubations (4°C) were performed with the primary antibodies: F1-ATPase (R-20, Santa Cruz Biotechnology), mtCK2 (R-15, Santa Cruz Biotechnology), cyt c (7H8.2C12) mAb (BD PharMingen), Ndufs3 complex I subunit (20C11) mAb (Invitrogen), VDAC (N-18, Santa Cruz Biotechnology). Secondary HRP-conjugated antibodies were detected by enhanced chemiluminescence (Amersham Biosciences). The baseline protein analysis was presented in Dufour et al. (Dufour et al., 2007), and is included here for interpretation.

Statistical Analysis

All data are presented as mean ± standard error of the mean (SE). Differences between mean values for cardiac weights (TAC and NAB trials), real-time PCR, and echocardiographic analysis were

determined by a two-way ANOVA followed by Bonferroni post hoc analysis with correction for multiple comparisons. For ^{31}P-NMR spectroscopic studies significant difference was determined by unpaired Student's t test. A p value of $\leq$ 0.05 was considered significantly different.

Supplemental Data

Supplemental Data include two tables and can be found with this article online at http://www.cellmetabolism.org/cgi/content/full/6/1/25/DC1/.

ACKNOWLEDGMENTS

Supported by NIH, K01 DK063051 (J.H.), the Canadian Institutes for Health Research (V.G.), and NIH, R01 HL058493 (D.K.). This research was supported (in part) by the Intramural Programs (NIEHS and NHLBI) of the NIH (E.M.). We acknowledge Washington University School of Medicine Diabetes Research Training Center (NIH, P60 DK20579), Siteman Cancer Center Multiplex Gene Analysis, and DRCC Pathology Cores for contributing to these studies. Special thanks to Bill Kraft for conducting electron microscopic analysis. We thank Mary Wingate for manuscript preparation.

Received: February 2, 2007
Revised: May 2, 2007
Accepted: June 18, 2007
Published: July 10, 2007

REFERENCES

Alaynick, W.A., Kondo, R.P., Xie, W., He, W., Dufour, C.R., Downes, M., Jonker, J.W., Giles, W., Naviaux, R.K., Giguère, V., and Evans, R.M. (2007). ERRγ directs and maintains the transition to oxidative metabolism in the postnatal heart. Cell Metab. *6*, this issue, 13–24.

Allard, M.F., Schonekess, B.O., Henning, S.L., English, D.R., and Lopaschuk, G.D. (1994). Contribution of oxidative metabolism and glycolysis to ATP production in hypertrophied hearts. Am. J. Physiol. *267*, H742–H750.

Anversa, P., Loud, A.V., Giacomelli, F., and Weiner, J. (1978). Absolute morphometric study of myocardial hypertrophy in experimental hypertension. II. Ultrastructure of myocytes and interstitium. Lab. Invest. *38*, 597–609.

Arany, Z., He, H., Lin, J., Hoyer, K., Handschin, C., Toka, O., Ahmad, F., Matsui, T., Chin, S., Wu, P.-H., et al. (2005). Transcriptional coactivator PGC-1α controls the energy state and contractile function of cardiac muscle. Cell Metab. *1*, 259–271.

Arany, Z., Novikov, M., Chin, S., Ma, Y., Rosenzweig, A., and Spiegelman, B.M. (2006). Transverse aortic constriction leads to accelerated heart failure in mice lacking PPARγ coactivator 1α. Proc. Natl. Acad. Sci. USA *103*, 10086–10091.

Ashrafian, H., Redwood, C., Blair, E., and Watkins, H. (2003). Hypertrophic cardiomyopathy: a paradigm for myocardial energy depletion. Trends Genet. *19*, 263–268.

Barrett, T., Troup, D.B., Wilhite, S.E., Ledoux, P., Rudnev, D., Evangelista, C., Kim, I.F., Soboleva, A., Tomashevsky, M., and Edgar, M. (2007). NCBI GEO: mining tens of millions of expression profiles–database and tools update. Nucleic Acids Res. *35*, D760–D765.

Bennett, M.J., Rinaldo, P., and Strauss, A.W. (2000). Inborn errors of mitochondrial fatty acid oxidation. Crit. Rev. Clin. Lab. Sci. *37*, 1–44.

Boudina, S., Sena, S., O'Neill, B.T., Tathireddy, P., Young, M.E., and Abel, E.D. (2005). Reduced mitochondrial oxidative capacity and increased mitochondrial uncoupling impair myocardial energetics in obesity. Circulation *112*, 2686–2695.

Carrier, J.C., Deblois, G., Champigny, C., Levy, E., and Giguere, V. (2004). Estrogen-related receptor α (ERRα) is a transcriptional regulator of apolipoprotein A-IV and controls lipid handling in the intestine. J. Biol. Chem. *279*, 52052–52058.

Christe, M.D., and Rodgers, R.L. (1994). Altered glucose and fatty acid oxidation in hearts of the spontaneously hypertensive rat. J. Mol. Cell. Cardiol. *26*, 1371–1375.

Cross, H., Murphy, E., and Steenbergen, C. (2002). Ca^{2+} loading and adrenergic stimulation reveal male/female differences in susceptibility to ischemia-reperfusion injury. Am. J. Physiol. *283*, H481–H489.

de las Fuentes, L., Herrero, P., Peterson, L.R., Kelly, D.P., Gropler, R.J., and Davila-Roman, V.G. (2003). Myocardial fatty acid metabolism: independent predictor of left ventricular mass in hypertension and in left ventricular dysfunction. Hypertension *41*, 83–87.

de Roos, A., Doornbos, J., Luyten, P., Oosterwaal, L., van der Wall, E., and den Hollander, J. (1992). Cardiac metabolism in patients with dilated and hypertrophic cardiomyopathy: Assessment with proton-decoupled P-31 MR spectroscopy. J. Magn. Reson. Imaging *2*, 711–719.

Dufour, C.R., Wilson, B.J., Huss, J.M., Kelly, D.P., Alaynick, W.A., Downes, M., Evans, R.M., Blanchette, M., and Giguère, V. (2007). Genome-wide orchestration of cardiac functions by orphan nuclear receptors ERRα and γ. Cell Metab. *5*, 345–356.

Finck, B.N., and Kelly, D.P. (2006). PGC-1 coactivators: Inducible regulators of energy metabolism in health and disease. J. Clin. Invest. *116*, 615–622.

Garnier, A., Fortin, D., Deloménie, C., Momken, I., Veksler, V., and Ventura-Clapier, R. (2003). Depressed mitochondrial transcription factors and oxidative capacity in rat failing cardiac and skeletal muscles. J. Physiol. *551*, 491–501.

Holmes, B.F., Sparling, D.P., Olson, A.L., Winder, W.W., and Dohm, G.L. (2005). Regulation of muscle GLUT4 enhancer factor and myocyte enhancer factor 2 by AMP-activated protein kinase. Am. J. Physiol. Endocrinol. Metab. *289*, 1071–1076.

Huss, J.M., and Kelly, D.P. (2005). Mitochondrial energy metabolism in heart failure: A question of balance. J. Clin. Invest. *115*, 547–555.

Huss, J.M., Kopp, R.P., and Kelly, D.P. (2002). PGC-1α coactivates the cardiac-enriched nuclear receptors estrogen-related receptor-α and -γ. J. Biol. Chem. *277*, 40265–40274.

Huss, J.M., Pinéda Torra, I., Staels, B., Giguère, V., and Kelly, D.P. (2004). ERRα directs PPARα signaling in the transcriptional control of energy metabolism in cardiac and skeletal muscle. Mol. Cell. Biol. *24*, 9079–9091.

Iemitsu, M., Miyazaki, H., Matsuda, M., and Yamaguchi, I. (2001). Physiological and pathological cardiac hypertrophy induce different molecular phenotypes in the rat. Am. J. Physiol. *281*, R2029–R2036.

Imahashi, K., Schneider, M.D., Steenbergen, C., and Murphy, E. (2004). Transgenic expression of Bcl-2 modulates energy metabolism, prevents cytosolic acidification during ischemia, and reduces ischemia/reperfusion injury. Circ. Res. *95*, 734–741.

Ingwall, J.S., Kramer, M.F., Fifer, M.A., Lorell, B.H., Shemin, R., Grossman, W., and Allen, P.D. (1985). The creatine kinase system in normal and diseased human myocardium. N. Engl. J. Med. *313*, 1050–1054.

Ingwall, J.S., and Weiss, R.G. (2004). Is the failing heart energy starved? On using chemical energy to support cardiac function. Circ. Res. *95*, 135–145.

Kayar, S.R., and Weiss, H.R. (1992). Diffusion distances, total capillary length, and mitochondrial volume in pressure overload myocardial hypertrophy. J. Mol. Cell. Cardiol. *24*, 1155–1166.

Kelly, D.P., and Strauss, A.W. (1994). Inherited cardiomyopathies. N. Engl. J. Med. *330*, 913–919.

Lehman, J.J., and Kelly, D.P. (2002). Gene regulatory mechanisms governing energy metabolism during cardiac hypertrophic growth. Heart Fail. Rev. *7*, 175–185.

Leone, T.C., Lehman, J.J., Finck, B.N., Schaeffer, P.J., Wende, A.R., Boudina, S., Courtois, M., Wozniak, D.F., Sambandam, N., Bernal-Mizrachi, C., et al. (2005). PGC-1α deficient mice exhibit multi-system

energy metabolic derangements: Muscle dysfunction, abnormal weight control, and hepatic steatosis. PLoS Biol. *3*, 672–687.

Lin, J., Handschin, C., and Spiegelman, B.M. (2005). Metabolic control through the PGC-1 family of transcription coactivators. Cell Metab. *1*, 361–370.

Luo, J., Sladek, R., Carrier, J., Bader, J.A., Richard, D., and Giguere, V. (2003). Reduced fat mass in mice lacking orphan nuclear receptor estrogen-related receptor alpha. Mol. Cell. Biol. *23*, 7947–7956.

Maloyan, A., Sanbe, A., Osinska, H., Westfall, M., Robinson, D., Imahashi, K.-I., Murphy, E., and Robbins, J. (2005). Mitochondrial dysfunction and apoptosis underlie the pathogenic process in α-B-crystallin desmin-related cardiomyopathy. Circulation *112*, 3451–3461.

Mootha, V.K., Handschin, C., Arlow, D., Xie, X., St.Pierre, J., Sihag, S., Yang, W., Altshuler, D., Puigserver, P., Patterson, N., et al. (2004). ERRα and Gabpa/b specify PGC-1α-dependent oxidative phosphorylation gene expression that is altered in diabetic muscle. Proc. Natl. Acad. Sci. USA *101*, 6570–6575.

Neubauer, S. (2007). The failing heart-an engine out of fuel. N. Engl. J. Med. *356*, 1140–1151.

Neubauer, S., Horn, M., Cramer, M., Harre, K., Newell, J.B., Peters, W., Pabst, T., Ertl, G., Hahn, D., Ingwall, J.S., et al. (1997). Myocardial phosphocreatine-to-ATP ratio is a predictor of mortality in patients with dilated cardiomyopathy. Circulation *96*, 2190–2196.

Palmieri, L., Alberio, S., Pisano, I., Lodi, T., Meznaric-Petrusa, M., Zidar, J., Santoro, A., Scarcia, P., Fontanesi, F., Lamantea, E., et al. (2005). Complete loss-of-function of the heart/muscle-specific adenine nucleotide translocator is associated with mitochondrial myopathy and cardiomyopathy. Hum. Mol. Genet. *14*, 3079–3088.

Rockman, H.A., Ross, R.S., Harris, A.N., Knowlton, K.U., Steinhelper, M.E., Field, L.J., Ross, J., Jr., and Chien, K.R. (1991). Segregation of atrial-specific and inducible expression of an atrial natriuretic factor transgene in an in vivo murine model of cardiac hypertrophy. Proc. Natl. Acad. Sci. USA *88*, 8277–8281.

Sack, M.N., Disch, D.L., Rockman, H.A., and Kelly, D.P. (1997). A role for Sp and nuclear receptor transcription factors in a cardiac hypertrophic growth program. Proc. Natl. Acad. Sci. USA *94*, 6438–6443.

Saks, V.A., Kuznetsov, A.V., Vendelin, M., Guerrero, K., Kay, L., and Seppet, E.K. (2004). Functional coupling as a basic mechanism of feedback regulation of cardiac energy metabolism. Mol. Cell. Biochem. *256–257*, 185–199.

Saks, V.A., Veksler, V.I., Kuznetsov, A.V., Kay, L., Sikk, P., Tiivel, T., Tranqui, L., Olivares, J., Winkler, K., Wiedemann, F., et al. (1998). Permeabilized cell and skinned fiber techniques in studies of mitochondrial function in vivo. Mol. Cell. Biochem. *184*, 81–100.

Sano, M., Wang, S.M., Shirai, M., Scaglia, F., Xie, M., Sakai, S., Tanaka, T., Kulkarni, P.A., Barger, P.M., Youker, K.A., et al. (2004). Activation of cardiac Cdk9 represses PGC-1 and confers a predisposition to heart failure. EMBO J. *23*, 3559–3569.

Schreiber, S.N., Emter, R., Hock, M.B., Knutti, D., Cardenas, J., Podvinec, M., Oakeley, E.J., and Kralli, A. (2004). The estrogen-related receptor alpha (ERRα) functions in PPARγ coactivator 1α (PGC-1α) - induced mitochondrial biogenesis. Proc. Natl. Acad. Sci. USA *101*, 6472–6477.

Schreiber, S.N., Knutti, D., Brogli, K., Uhlmann, T., and Kralli, A. (2003). The transcriptional coactivator PGC-1 regulates the expression and activity of the orphan nuclear receptor estrogen-related receptor α (ERRα). J. Biol. Chem. *278*, 9013–9018.

Strøm, C.C., Aplin, M., Ploug, T., Christoffersen, T.E.H., Langfort, J., Viese, M., Galbo, H., Haunso, S., and Sheikh, S.P. (2005). Expression profiling reveals differences in metabolic gene expression between exercise-induced cardiac effects and maladaptive cardiac hypertrophy. FEBS J. *272*, 2684–2695.

Taegtmeyer, H., Razeghi, P., and Young, M.E. (2002). Mitochondrial proteins in hypertrophy and atrophy: A transcript analysis in rat heart. Clin. Exp. Pharmacol. Physiol. *29*, 346–350.

Tian, R., and Abel, E.D. (2001). Responses of GLUT4-deficient hearts to ischemia underscore the importance of glycolysis. Circulation *103*, 2961–2966.

Tian, R., Nascimben, L., Kaddurah-Daouk, R., and Ingwall, J.S. (1996). Depletion of energy reserve via the creatine kinase reaction during the evolution of heart failure in cardiomyopathic hamsters. J. Mol. Cell. Cardiol. *28*, 755–765.

Vakili, B.A., Okin, P.M., and Devereux, R.B. (2001). Prognostic implications of left ventricular hypertrophy. Am. Heart J. *141*, 334–341.

Villena, J.A., Hock, M.B., Chang, W.Y., Barcas, J.E., Giguère, V., and Kralli, A. (2007). Orphan nuclear receptor estrogen-related receptor α is essential for adaptive thermogenesis. Proc. Natl. Acad. Sci. USA *104*, 1418–1423.

Wallace, D.C. (2000). Mitochondrial defects in cardiomyopathy and neuromuscular disease. Am. Heart J. *139*, S70–S85.

Weiss, R.G., Chatham, J.C., Charron, M.J., Georgakopolous, D., Wallimann, T., Kay, L., Walzel, B., Wang, Y., Kass, D.A., Gerstenblith, G., et al. (2002). An increase in the myocardial PCr/ATP ratio in GLUT4 null mice. FASEB J. *16*, 613–615.

Weiss, R.G., Gerstenblith, G., and Bootomley, P.A. (2005). ATP flux through creatine kinase in the normal, stressed, and failing human heart. Proc. Natl. Acad. Sci. USA *102*, 808–813.

Wende, A.R., Huss, J.M., Schaeffer, P.J., Giguère, V., and Kelly, D.P. (2005). PGC-1α coactivates PDK4 gene expression via the orphan nuclear receptor ERRα: A mechanism for transcriptional control of muscle glucose metabolism. Mol. Cell. Biol. *25*, 10684–10694.

Ye, Y., Wang, C., Zhang, J., Cho, Y.K., Gong, G., Murakami, Y., and Bache, R.J. (2001). Myocardial creatine kinase kinetics and isoform expression in hearts with severe LV hypertrophy. Am. J. Physiol. Heart Circ. Physiol. *281*, 376–386.